Additive-Free Formic Acid Dehydrogenation Catalyzed by a Cobalt Complex†.

Nicolas Lentz, Alicia Aloisi, Pierre Thuéry, Emmanuel Nicolas and Thibault Cantat*

Université Paris-Saclay, CEA, CNRS, NIMBE, 91191, Gif-sur-Yvette, France. E-mail: thibault.cantat@cea.fr

ABSTRACT: The reversible storage of hydrogen through the intermediate formation of Formic Acid (FA) is a promising solution to its safe transport and distribution. However, the common necessity of using bases or additives in the catalytic dehydrogenation of FA is a limitation. In this context, two new cobalt complexes (**1** and **2**) were synthesized with a pincer PP(NH)P ligand containing a phosphoramine moiety. Their reaction with an excess FA yields a cobalt(I)-hydride complex (**3**). We report here the unprecedented catalytic activity of **3** in the dehydrogenation of FA, with a turnover frequency (TOF) of 67 min^{-1} measured in the first minute and a turnover number (TON) of 454, without the need for bases or additives. A mechanistic study reveals the existence of ligand-metal cooperativity with intermolecular hydrogen bonding, also influenced by the concentration of formic acid.

The share of renewable energies in the European energetic mix has never been higher, reaching 13.9 % in 2017.[1] However, with their increased penetration, the long-term storage of intermittent energies becomes more and more urgent, in order to accommodate for seasonal variations in production and consumption.[2] Hydrogen is a promising energy carrier for that purpose, as it is readily available and has a high energy density; but its storage as a compressed gas is still problematic.[3] Chemicals such as Formic Acid (FA) can act as Liquid Organic Hydrogen Carriers (LOHCs) through hydrogenation and dehydrogenation cycles.[4-8]

The catalytic dehydrogenation of FA has been extensively studied during the past decade. Several homogeneous complexes, based on noble metals such as iridium,[9-11] rhodium,[12-14] molybdenum,[15] ruthenium[16-19] and osmium[20] have been reported as catalysts for this reaction. These studies demonstrated that the ligand architecture has a crucial impact on the catalyst activity and stability and therefore governs the catalysts turnover number (TON) and turnover frequency (TOF). In parallel, several groups developed catalysts based on the use of 3d group metals as a promising alternative to expensive and potentially rare noble metals. Yet, this substitution often comes at the price of a decrease reactivity and stability.[21] Beller *et al.* pioneered the use of iron complexes in 2010, and a number of PNP pincer ligands chelated to an iron centre have been reported since.[22-31] Manganese complexes have also been reported to be active in this reaction, as reported by Boncella and Tondreau *et al.*, and Beller *et al.*.[32-34] The activity of other 3d metals was assessed over the past few years, using nickel (Junge, Enthaler *et al.* and Parkin *et al.*),[35, 36] copper (Correa *et al.*),[37] and cobalt (Beller *et al.* and Onishi *et al.*).[38, 39] Group 13 compounds were also investigated, namely aluminium by the group of Berben in 2014,[40] and boron by our group.[41]

The presence of participative ligands is a consistent feature in the majority of the reported examples, to include an internal base in the coordination sphere of the catalyst to activate FA.[42-45] A second feature of interest, especially in the case of 3d group metals, is that an external base or additives such as BF_4 salts are often necessary to retain a catalytic activity.[46] We recently reported a new ligand featuring an N–H moiety on a triphosphane backbone that helped stabilizing copper hydride complexes.[47] This chelating ligand presents a phosphoramine function (R_2P-NHR') together with two phosphines, which can act as a pendant amine and a participative ligand. It is hence an excellent platform to design catalysts for the dehydrogenation of formic acid. Herein, we report the coordination properties of this new PP(NH)P ligand with cobalt, and describe the synthesis of two PP(NH)P–Co(II) complexes, **1** and **2**, and a PP(NH)P–Co(I)–H complex, **3**. The catalytic activity of all three complexes in the dehydrogenation of formic acid was investigated, and a theoretical mechanistic study unveiled the role of the ligand in the remarkable activity of **3**.

The PP(NH)P ligand was prepared following the literature procedure,[47] and its coordination was investigated with two different cobalt precursors (Scheme 1): cobalt(II) chloride or cobalt(II) acetate were readily coordinated by the PP(NH)P ligand in a THF solution at 80 °C, to yield complexes **1** and **2** respectively, which were isolated quantitatively as brown powders. Both complexes are paramagnetic,[48] which prevented any conclusive NMR analysis, but single crystals of **1**·THF were obtained from the evaporation of a saturated THF solution (Figure 1a). All efforts towards crystallization of **2** remained unfruitful. In the molecular structure of **1**, the cobalt atom adopts a distorted square pyramidal geometry ($\tau = 0.18$)[49] with a chlorine atom in the axial position and the phosphine and second chlorine ligands in the basal positions. An hydrogen bond was observed between one chlorine atom and the phosphoramide hydrogen, as expected for such a participative ligand.

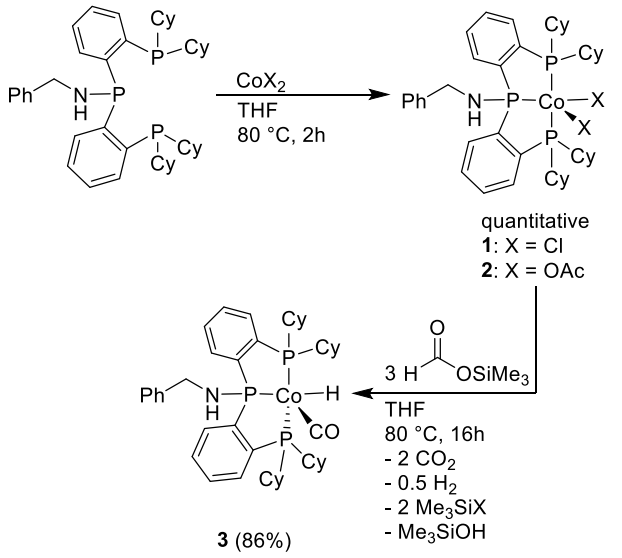

Scheme 1: Synthesis of Co-complexes **1**, **2** and **3**.

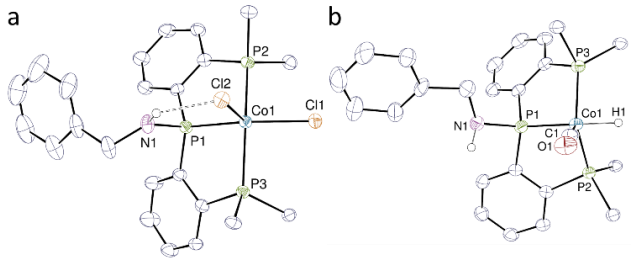

Figure 1: (a) Molecular structure of **1**. Carbon-bound hydrogen atoms and cyclohexyl rings have been omitted. The hydrogen bond is shown as a dashed line. Selected bond distances (Å) and bond angles (°): P1−N1 1.660(4); P1−Co1 2.1397(12); P2−Co1 2.2444(12); P3−Co1 2.2775(12); Cl1−Co1 2.2526(11); Cl2−Co1 2.4132(11); Cl1−Co1−Cl2 98.24(4); Cl1−Co1−P1 167.45(5); Cl1−Co1−P2 91.90(4); Cl1−Co1−P3 92.30(4); Cl2−Co1−P1 94.30(4); Cl2−Co1−P2 100.08(4); Cl2−Co1−P3 102.36(4); P2−Co1−P3 156.32(5); P1−Co1−P2 86.28(4); P1−Co1−P3 84.59(4). (b): Molecular structure of **3**. Carbon-bound hydrogen atoms and cyclohexyl rings have been omitted. Selected bond distances (Å) and bond angles (°): P1−N1 1.705(2); P1−Co1 2.1224(7); P2−Co1 2.1528(7); P3−Co1 2.1540(7); H1−Co1 1.46(3); C1−Co1 1.731(3); C1−O1 1.163(3); C1−Co1−H1 91.4(11); C1−Co1−P1 104.71(8); C1−Co1−P2 111.99(8); C1−Co1−P3 120.07(8); H1−Co1−P1 163.4(11); H1−Co1−P2 82.3(11); H1−Co1−P3 87.9(10); P2−Co1−P3 127.16(3); P1−Co1−P2 87.74(3); P1−Co1−P3 87.60(3).

The reactivity of both Co(II) complexes **1** and **2** was investigated with 5 equivalents of formic acid for 2 h at 150 °C. ^{1}H NMR showed the total conversion of formic acid, together with the formation of a new diamagnetic complex, **3**, featuring two singlets at 97.2 and 159.7 ppm in ^{31}P{^{1}H} NMR and a characteristic doublet of triplet at –10.91 ppm in ^{1}H NMR., indicative of a cobalt(I) hydride complex. In addition, GC analysis of the headspace showed the selective conversion of FA into CO_2 and H_2, and no CO could be detected. Although **3** could not be isolated pure from stoichiometric reactions between **1** or **2** and **2** equiv. FA, it was successfully prepared by replacing FA with a surrogate which cannot undergo dehydrogenation reactions: trimethylsilylformate. Complexes **1** and **2** both reacted with 3 equiv. TMS-OCHO, to give, after 16h at 80 °C, Co^{I} complex **3** as an orange solid in 86% yield (Scheme 1). Crystals of **3**·2.5dioxane were obtained from a saturated 1,4-dioxane solution (Figure 1b) and confirmed the presence of the hydride, together with a carbonyl ligand. In the molecular structure of **3**, the cobalt atom adopts a distorted trigonal bipyramidal geometry (τ = 0.60) with the central phosphorus and the hydride in the axial positions (H1−Co1−P1 = 163.4(11) °) and the remaining phosphines and carbon monoxide in the equatorial positions, similar to previously reported hydrido carbonyl cobalt complexes.[50-52] The Co1−H1 and Co1−C1 bonds are typical of such structures, with lengths of 1.46(3) and 1.731(3) Å respectively and comparable to those found in [Co(CO)H(PPh$_3$)$_3$] (1.41(9) and 1.704(17) Å).[50]

The catalytic activities of complexes **1**, **2** and **3** were finally investigated in the dehydrogenation of FA at 80 °C in 1,4-dioxane, with 0.5 mol% loading (Figure 2, top). While **1** was found inactive at 80 °C, **2** reached a production of 79 mL of gas after 20 min, corresponding to a TON of 165. On the other hand, **3** reached full conversion after only 10 min of reaction. Interestingly, an induction period was observed with **2** in the first minute of the catalysis, suggesting that **2** might be converted to the active species, supposedly **3**, according to the reactivity noted hereabove. In fact, **3** was observed as the major species, after decomposition of FA with **2**. Both **2** and **3** have unprecedented activities for homogeneous cobalt complexes with TON$_{1h}$ = 165 and 200, compared to the MACHO ligand-bound cobalt-based catalyst reported by Beller *et al.* in the absence of any additive (no activity reported) or base (TON$_{1h}$ = 29 with 2 equiv. of NaBEt$_3$H with respect to the complex).[39]

Catalyst **3** reached a full conversion of FA within the first 10 min of the reaction with a TOF of 67 min^{-1} (Table 1, entry 1). The catalyst was not only active in dioxane, but also in toluene (TON$_{1h}$ = 154, TOF$_{1min}$ = 4 min^{-1}) or even in protic solvents, incl. water (TON$_{1h}$ = 102, TOF$_{1min}$ = 13 min^{-1}), although a diminished stability and activity were noted in both cases (Table 1, entries 1, 2 and 3). The impact of the solvent on the activity and stability of **3** might result from its influence on the solubility of the complexes as well as heterolytic bond cleavage and stabilization of ionic intermediates.[53, 54] Finally, halving or doubling the FA concentration led to decreased kinetics with lower TOF$_{1min}$ (19 or 13 min^{-1} respectively, vs. 67 min^{-1} at 1M) (Table 1, entries 1, 4 and 5), suggesting either a complex rate order for FA or an intermolecular decomposition pathway.

Table 1. FA dehydrogenation catalysed by **3**.

Entry	Solvent (Conc mol.L^{-1})	V$_{1min}$ (mL)	V$_{1h}$ (mL)	TON$_{1h}$	TOF$_{1min}$ (min^{-1})
1	1,4-dioxane (1)	32	96	200	67
2	Water (1)	6	49	102	13
3	Toluene (1)	2	74	154	4
4	1,4-dioxane (2)	6	49	106	13
5	1,4-dioxane (0.5)	9	79	169	19

Conditions: FA (2 mmol) in solvent and **3** (0.5 mol%) at 80 °C.

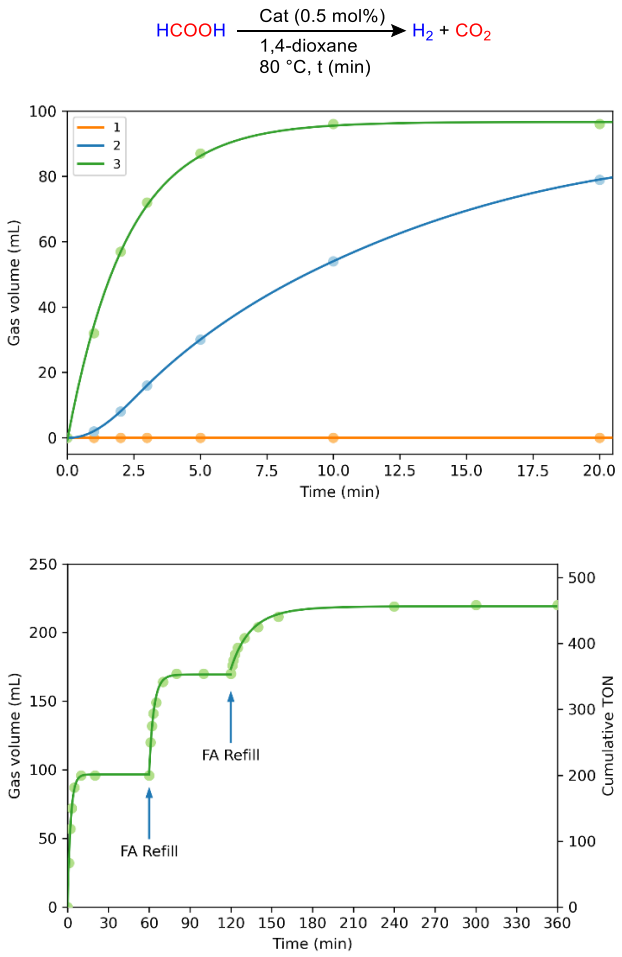

Figure 2: top: Kinetic profile dehydrogenation of FA catalyzed by complexes **1**, **2** and **3**. Bottom: Kinetic profile for the dehydrogenation of FA catalyzed by **3**. Reaction conditions: FA (2 mmol) in 1,4-dioxane (2 mL) and catalyst (0.5 mol%) at 80 °C. Gas evolution was measured with a graduated cylinder (see ESI for details).

To get a deeper insight into the mechanism, the reaction was computed, and the most favoured pathway is depicted in Scheme 2. Cobalt complex **A**, an isomer of **3** (see ESI), deprotonates an incoming molecule of FA and releases H_2 through $\mathbf{TS_{AB}}$, to yield the intermediate formate complex **B** ($\mathbf{TS_{AB}}$: 11.9 kcal.mol^{-1}, ΔG = -4.7 kcal.mol^{-1}). The decarboxylation of **B** to regenerate **A**, after release of CO_2, involves in contrast several steps. While a direct β-H elimination can be considered ($\mathbf{TS_{BD}}$, 16.3 kcal.mol^{-1}), formate complex **B** was found to readily insert a second molecule of FA in the Co–OCHO bond, via $\mathbf{TS_{BC}}$ (1.0 kcal.mol^{-1}). The resulting complex **C** then includes a formato ligand, which is coordinated to the Co^{I} ion *via* its C–H bond and stabilized through H-bonding with the N–H moiety of the phosphoramine ligand and a FA molecule. **C** is 2.3 kcal.mol^{-1} higher in energy than **A**. After release of FA, intermediate **D** is formed, which features an H-bound formate complex, H-bonded to the participative ligand. A complex similar to **D** has also been described by Hazari, Schneider *et al.*.[26] The subsequent decarboxylation of the formato ligand in **D** occurs through $\mathbf{TS_{DA}}$ (18.7 kcal.mol^{-1}, $\Delta\Delta G_{DA}$ = -19.2 kcal.mol^{-1}) and closes the catalytic cycle, while the overall dehydrogenation reaction is exergonic (ΔG = -9.5 kcal.mol^{-1}). The total energetic span of the reaction, 23.4 kcal.mol^{-1}, is defined by the resting state **B** and the decarboxylation step ($\mathbf{TS_{DA}}$), which is the rate-determining step. This value is consistent with our observations of a fast reaction at 80 °C. Moreover, the non-trivial influence of the concentration in FA on the reaction rate can be rationalized with the necessity to involve two molecules of FA in the process, the first one being involved in the dehydrogenation and the second one in the decarboxylation. Interestingly, in this mechanism, the participative ligand is never deprotonated, and only acts as hydrogen bond donor.

Finally, in order to push the reaction towards a maximum TON while keeping high TOF throughout the reaction by a control of the amount of FA, a reloading experiment was set up using **3** in 1,4-dioxane (Figure 2, bottom). We observed the deactivation of the catalyst through a simultaneous decrease in TON and TOF upon each refill (TOF_{1min} were 67, 50 and 13 min^{-1} at each FA loading). It was however possible to reach a total TON of 458 over the course of a 4 hour reaction.

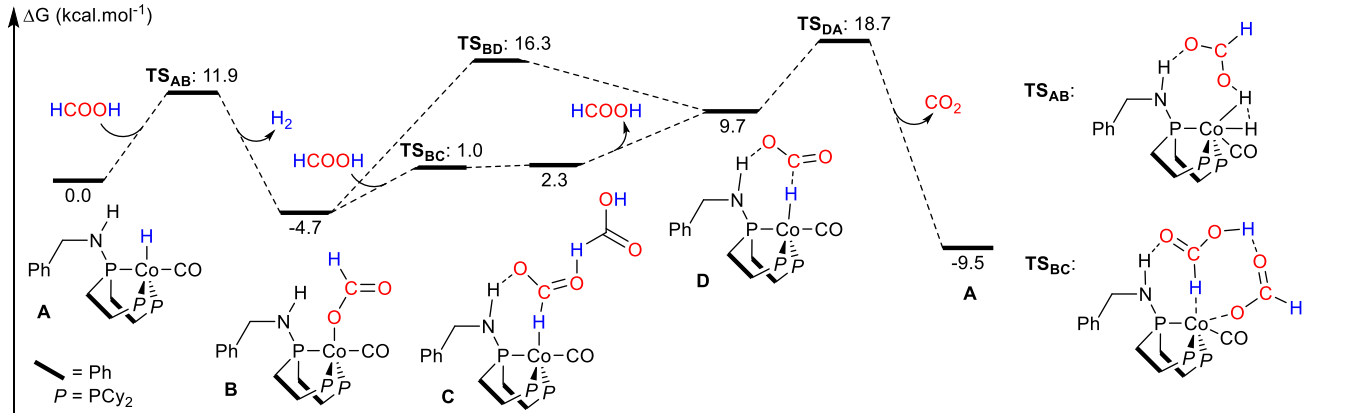

Scheme 2: Computed reaction profile for the **Co-1** catalyzed formic acid dehydrogenation reaction. Computations parameters: Gaussian 16 Rev C.01; ω-B97X-D/Def2-TZVP (Co), 6-311+G(d,p) (mobile H) 6-31G(d) (other atoms), SMD (Solvent: 1,4-dioxane).

In conclusion, we described herein the synthesis of new cobalt(II) and cobalt(I) complexes, supported by a chelating participative ligand possessing a phosphoramine arm. The activity of the complexes was tested in the dehydrogenation of FA. The cobalt(I) hydrido carbonyl complex **3** was found highly reactive, pushing further the activity of homogeneous 3d metal, by reaching TOF values of 67 min^{-1} and a TON_{max} of 458. It is, to the best of our knowledge, the first report of a cobalt catalyst active in the dehydrogenation of FA without addition of bases or additives. DFT calculations helped rationalizing the importance of the participative ligand and the concentration of FA, in accordance with the experimental results. Further developments for this catalytic system could involve its implementation in a continuous FA injection device, in order to keep the FA concentration as constant as possible.

ASSOCIATED CONTENT

Supporting Information

The Supporting Information is available free of charge on the ACS Publications website. Synthesis, characterizations, crystal structure refinements and computational investigations (PDF). Cartesian coordinates of all computed structures (XYZ file)

ACCESSION CODES

‡ CCDC numbers: 2011895 and 2011896 contain the supplementary crystallographic data for this paper. These data can be obtained free of charge from The Cambridge Crystallographic Data Centre via www.ccdc.cam.ac.uk/data_request/cif

AUTHOR INFORMATION

Corresponding Author

* **Thibault Cantat** – Université Paris-Saclay, CEA, CNRS, NIMBE, 91191, Gif-sur-Yvette, France.
E-mail: thibault.cantat@cea.fr.

Authors

Nicolas Lentz – Université Paris-Saclay, CEA, CNRS, NIMBE, 91191, Gif-sur-Yvette, France.
Alicia Aloisi – Université Paris-Saclay, CEA, CNRS, NIMBE, 91191, Gif-sur-Yvette, France.
Pierre Thuéry – Université Paris-Saclay, CEA, CNRS, NIMBE, 91191, Gif-sur-Yvette, France.
Emmanuel Nicolas – Université Paris-Saclay, CEA, CNRS, NIMBE, 91191, Gif-sur-Yvette, France.

Notes

The authors declare no competing financial interest.

ACKNOWLEDGMENT

The authors acknowledge for financial support of this work: CEA, CNRS, CINES (project sis6494), the CHARMMMAT Laboratory of Excellence, the European Research Council (ERC Consolidator Grant Agreement no. 818260), ADEME (fellowship to AA). This research was supported by the European Union's Horizon 2020 Research and Innovation Programme under grant agreement no. 768919, Carbon4PUR project.

REFERENCES

1. Energy, transport and environment statistics; Eurostat2019.
2. Kerskes, H., Chapter 17 - Thermochemical Energy Storage. In Storing Energy, Letcher, T. M., Ed. Elsevier: Oxford, 2016; pp 345-372.
3. Züttel, A.; Borgschulte, A.; Schlapbach, L., Hydrogen as a Future Energy Carrier. Wiley-VCH2008.
4. Züttel, A.; Hirscher, M.; Panella, B.; Yvon, K.; Orimo, S.-i.; Bogdanović, B.; Felderhoff, M.; Schüth, F.; Borgschulte, A.; Goetze, S.; Suda, S.; Kelly, M. T., Hydrogen Storage. In Hydrogen as a Future Energy Carrier,2008; pp 165-263.
5. Sordakis, K.; Tang, C.; Vogt, L. K.; Junge, H.; Dyson, P. J.; Beller, M.; Laurenczy, G., Homogeneous Catalysis for Sustainable Hydrogen Storage in Formic Acid and Alcohols. Chem. Rev. **2018,** 118, 372-433.
6. Li, Z.; Xu, Q., Metal-Nanoparticle-Catalyzed Hydrogen Generation from Formic Acid. Acc. Chem. Res. **2017,** 50, 1449-1458.
7. Onishi, N.; Laurenczy, G.; Beller, M.; Himeda, Y., Recent progress for reversible homogeneous catalytic hydrogen storage in formic acid and in methanol. Coord. Chem. Rev. **2018,** 373, 317-332.
8. Mellmann, D.; Sponholz, P.; Junge, H.; Beller, M., Formic acid as a hydrogen storage material – development of homogeneous catalysts for selective hydrogen release. Chem. Soc. Rev. **2016,** 45, 3954-3988.
9. Lu, S.-M.; Wang, Z.; Wang, J.; Li, J.; Li, C., Hydrogen generation from formic acid decomposition on a highly efficient iridium catalyst bearing a diaminoglyoxime ligand. Green Chem. **2018,** 20, 1835-1840.
10. Papp, G.; Ölveti, G.; Horváth, H.; Kathó, Á.; Joó, F., Highly efficient dehydrogenation of formic acid in aqueous solution catalysed by an easily available water-soluble iridium(iii) dihydride. Dalton Trans. **2016,** 45, 14516-14519.
11. Celaje, J. J. A.; Lu, Z.; Kedzie, E. A.; Terrile, N. J.; Lo, J. N.; Williams, T. J., A prolific catalyst for dehydrogenation of neat formic acid. Nature Comm. **2016,** 7, 11308.
12. Wang, Z.; Lu, S.-M.; Wu, J.; Li, C.; Xiao, J., Iodide-Promoted Dehydrogenation of Formic Acid on a Rhodium Complex. Eur. J. Inorg. Chem. **2016,** 2016, 490-496.
13. Fink, C.; Laurenczy, G., CO_2 as a hydrogen vector – transition metal diamine catalysts for selective HCOOH dehydrogenation. Dalton Trans. **2017,** 46, 1670-1676.
14. Fink, C.; Laurenczy, G., A Precious Catalyst: Rhodium-Catalyzed Formic Acid Dehydrogenation in Water. Eur. J. Inorg. Chem. **2019,** 2019, 2381-2387.
15. Neary, M. C.; Parkin, G., Dehydrogenation, disproportionation and transfer hydrogenation reactions of formic acid catalyzed by molybdenum hydride compounds. Chem. Sci. **2015,** 6, 1859-1865.
16. Czaun, M.; Goeppert, A.; Kothandaraman, J.; May, R. B.; Haiges, R.; Prakash, G. K. S.; Olah, G. A., Formic Acid As a Hydrogen Storage Medium: Ruthenium-Catalyzed Generation of Hydrogen from Formic Acid in Emulsions. ACS Catal. **2014,** 4, 311-320.
17. Pan, Y.; Pan, C.-L.; Zhang, Y.; Li, H.; Min, S.; Guo, X.; Zheng, B.; Chen, H.; Anders, A.; Lai, Z.; Zheng, J.; Huang, K.-W., Selective Hydrogen Generation from Formic Acid with Well-Defined Complexes of Ruthenium and Phosphorus–Nitrogen PN3-Pincer Ligand. Chem. Asian. J. **2016,** 11, 1357-1360.
18. Mellone, I.; Bertini, F.; Peruzzini, M.; Gonsalvi, L., An active, stable and recyclable Ru(ii) tetraphosphine-based catalytic system for hydrogen production by selective formic acid dehydrogenation. Catal. Sci. Tech. **2016,** 6, 6504-6512.
19. Anderson, N. H.; Boncella, J. M.; Tondreau, A. M., Reactivity of Silanes with (tBuPONOP)Ruthenium Dichloride: Facile Synthesis of Chloro-Silyl Ruthenium Compounds and Formic Acid Decomposition. Chem. Eur. J. **2017,** 23, 13617-13622.
20. Esteruelas, M. A.; García-Yebra, C.; Martín, J.; Oñate, E., Dehydrogenation of Formic Acid Promoted by a Trihydride-Hydroxo-Osmium(IV) Complex: Kinetics and Mechanism. ACS Catal. **2018,** 8, 11314-11323.

21. Guan, C.; Pan, Y.; Zhang, T.; Ajitha, M. J.; Huang, K.-W., An Update on Formic Acid Dehydrogenation by Homogeneous Catalysis. Chem. Asian. J. **2020,** 15, 937-946.
22. Boddien, A.; Gärtner, F.; Jackstell, R.; Junge, H.; Spannenberg, A.; Baumann, W.; Ludwig, R.; Beller, M., ortho-Metalation of Iron(0) Tribenzylphosphine Complexes: Homogeneous Catalysts for the Generation of Hydrogen from Formic Acid. Angew. Chem. Int. Ed. **2010,** 49, 8993-8996.
23. Boddien, A.; Loges, B.; Gärtner, F.; Torborg, C.; Fumino, K.; Junge, H.; Ludwig, R.; Beller, M., Iron-Catalyzed Hydrogen Production from Formic Acid. J. Am. Chem. Soc. **2010,** 132, 8924-8934.
24. Boddien, A.; Mellmann, D.; Gärtner, F.; Jackstell, R.; Junge, H.; Dyson, P. J.; Laurenczy, G.; Ludwig, R.; Beller, M., Efficient Dehydrogenation of Formic Acid Using an Iron Catalyst. Science **2011,** 333, 1733.
25. Zell, T.; Butschke, B.; Ben-David, Y.; Milstein, D., Efficient Hydrogen Liberation from Formic Acid Catalyzed by a Well-Defined Iron Pincer Complex under Mild Conditions. Chem. Eur. J. **2013,** 19, 8068-8072.
26. Bielinski, E. A.; Lagaditis, P. O.; Zhang, Y.; Mercado, B. Q.; Würtele, C.; Bernskoetter, W. H.; Hazari, N.; Schneider, S., Lewis Acid-Assisted Formic Acid Dehydrogenation Using a Pincer-Supported Iron Catalyst. J. Am. Chem. Soc. **2014,** 136, 10234-10237.
27. Zell, T.; Milstein, D., Hydrogenation and Dehydrogenation Iron Pincer Catalysts Capable of Metal–Ligand Cooperation by Aromatization/Dearomatization. Acc. Chem. Res. **2015,** 48, 1979-1994.
28. Mellone, I.; Gorgas, N.; Bertini, F.; Peruzzini, M.; Kirchner, K.; Gonsalvi, L., Selective Formic Acid Dehydrogenation Catalyzed by Fe-PNP Pincer Complexes Based on the 2,6-Diaminopyridine Scaffold. Organometallics **2016,** 35, 3344-3349.
29. Curley, J. B.; Bernskoetter, W. H.; Hazari, N., Additive-Free Formic Acid Dehydrogenation Using a Pincer-Supported Iron Catalyst. ChemCatChem **2020,** 12, 1934-1938.
30. Bertini, F.; Mellone, I.; Ienco, A.; Peruzzini, M.; Gonsalvi, L., Iron(II) Complexes of the Linear rac-Tetraphos-1 Ligand as Efficient Homogeneous Catalysts for Sodium Bicarbonate Hydrogenation and Formic Acid Dehydrogenation. ACS Catal. **2015,** 5, 1254-1265.
31. Montandon-Clerc, M.; Dalebrook, A. F.; Laurenczy, G., Quantitative aqueous phase formic acid dehydrogenation using iron(II) based catalysts. J. Catal. **2016,** 343, 62-67.
32. Tondreau, A. M.; Boncella, J. M., 1,2-Addition of Formic or Oxalic Acid to –N{CH2CH2(PiPr2)}2-Supported Mn(I) Dicarbonyl Complexes and the Manganese-Mediated Decomposition of Formic Acid. Organometallics **2016,** 35, 2049-2052.
33. Anderson, N. H.; Boncella, J.; Tondreau, A. M., Manganese-Mediated Formic Acid Dehydrogenation. Chem. Eur. J. **2019,** 25, 10557-10560.
34. Léval, A.; Agapova, A.; Steinlechner, C.; Alberico, E.; Junge, H.; Beller, M., Hydrogen production from formic acid catalyzed by a phosphine free manganese complex: investigation and mechanistic insights. Green Chem. **2020,** 22, 913-920.
35. Enthaler, S.; Brück, A.; Kammer, A.; Junge, H.; Irran, E.; Gülak, S., Exploring the Reactivity of Nickel Pincer Complexes in the Decomposition of Formic Acid to CO_2/H_2 and the Hydrogenation of $NaHCO_3$ to HCOONa. ChemCatChem **2015,** 7, 65-69.
36. Neary, M. C.; Parkin, G., Nickel-catalyzed release of H_2 from formic acid and a new method for the synthesis of zerovalent $Ni(PMe_3)_4$. Dalton Trans. **2016,** 45, 14645-14650.
37. Correa, A.; Cascella, M.; Scotti, N.; Zaccheria, F.; Ravasio, N.; Psaro, R., Mechanistic insights into formic acid dehydrogenation promoted by Cu-amino based systems. Inorg. Chim. Acta **2018,** 470, 290-294.
38. Onishi, M., Decomposition of formic acid catalyzed by hydrido (phosphonite) cobalt (I) under photoirradiation. J. Mol. Catal. **1993,** 80, 145-149.
39. Zhou, W.; Wei, Z.; Spannenberg, A.; Jiao, H.; Junge, K.; Junge, H.; Beller, M., Cobalt-Catalyzed Aqueous Dehydrogenation of Formic Acid. Chem. Eur. J. **2019,** 25, 8459-8464.
40. Myers, T. W.; Berben, L. A., Aluminium–ligand cooperation promotes selective dehydrogenation of formic acid to H_2 and CO_2. Chem. Sci. **2014,** 5, 2771-2777.
41. Chauvier, C.; Tlili, A.; Das Neves Gomes, C.; Thuéry, P.; Cantat, T., Metal-free dehydrogenation of formic acid to H_2 and CO_2 using boron-based catalysts. Chem. Sci. **2015,** 6, 2938-2942.
42. Khusnutdinova, J. R.; Milstein, D., Metal–Ligand Cooperation. Angew. Chem. Int. Ed. **2015,** 54, 12236-12273.
43. Zhao, B.; Han, Z.; Ding, K., The N□H Functional Group in Organometallic Catalysis. Angew. Chem. Int. Ed. **2013,** 52, 4744-4788.
44. Agapova, A.; Alberico, E.; Kammer, A.; Junge, H.; Beller, M., Catalytic Dehydrogenation of Formic Acid with Ruthenium-PNP-Pincer Complexes: Comparing N-Methylated and NH-Ligands. ChemCatChem **2019,** 11, 1910-1914.
45. Alig, L.; Fritz, M.; Schneider, S., First-Row Transition Metal (De)Hydrogenation Catalysis Based On Functional Pincer Ligands. Chem. Rev. **2019,** 119, 2681-2751.
46. For instance, $LiBF_4$ can react as a Lewis acid either as a source of BF_3 or through the Li^+ cation, or by itself through the BF_4 anion.
47. Aloisi, A.; Crochet, E.; Nicolas, E.; Berthet, J.-C.; Lescot, C.; Thuéry, P.; Cantat, T., Copper–Ligand Cooperativity in H_2 Activation Enables the Synthesis of Copper Hydride Complexes. Under Revision **2020**.
48. No peak were observed in the paramagnetic regions as well.
49. Crans, D. C.; Chen, H.; Anderson, O. P.; Miller, M. M., Vanadium(V)-protein model studies: solid-state and solution structure. J. Am. Chem. Soc. **1993,** 115, 6769-6776.
50. Whitfield, J. M.; Watkins, S. F.; Tupper, G. B.; Baddley, W. H., Preparation and crystal structure of trans-carbonylhydridotris(triphenylphosphine)cobalt(I): a quantitative assessment of trigonal bipyramidal geometry. J. Chem. Soc., Dalton Trans. **1977**, 407-413.
51. Lagaditis, P. O.; Schluschaß, B.; Demeshko, S.; Würtele, C.; Schneider, S., Square-Planar Cobalt(III) Pincer Complex. Inorg. Chem. **2016,** 55, 4529-4536.
52. Fu, S.; Chen, N.-Y.; Liu, X.; Shao, Z.; Luo, S.-P.; Liu, Q., Ligand-Controlled Cobalt-Catalyzed Transfer Hydrogenation of Alkynes: Stereodivergent Synthesis of Z- and E-Alkenes. J. Am. Chem. Soc. **2016,** 138, 8588-8594.
53. Heimann, J. E.; Bernskoetter, W. H.; Hazari, N.; Mayer, James M., Acceleration of CO_2 insertion into metal hydrides: ligand, Lewis acid, and solvent effects on reaction kinetics. Chem. Sci. **2018,** 9, 6629-6638.
54. Heimann, J. E.; Bernskoetter, W. H.; Hazari, N., Understanding the Individual and Combined Effects of Solvent and Lewis Acid on CO_2 Insertion into a Metal Hydride. J. Am. Chem. Soc. **2019,** 141, 10520-10529.